energies

MDPI

Article

On the Crystal Chemistry of Photochromic Yttrium Oxyhydride

Magnus H. Sørby *, Fredrik Martinsen, Smagul Zh. Karazhanov, Bjørn C. Hauback and Erik S. Marstein

Institute for Energy Technology, P.O. Box 40, 2027 Kjeller, Norway; fredrikamartinsen@gmail.com (F.M.); smagul.karazhanov@ife.no (S.Z.K.); bjorn.hauback@ife.no (B.C.H.); erik.stensrud.marstein@ife.no (E.S.M.)
* Correspondence: magnus.sorby@ife.no

Abstract: Yttrium oxyhydride exhibits photochromic properties at ambient temperature and pressures. Although oxygen plays an important role in determining the optoelectronic properties of the material, the question remains open regarding the site that it occupies in the crystal structure. In this paper, we address the issue by synchrotron radiation and neutron powder diffraction measurements. We report that the oxide anions occupy tetrahedral sites together with hydride anions in the face-centered cubic structure.

Keywords: yttrium hydride; oxyhydride; photochromic materials

Citation: Sørby, M.H.; Martinsen, F.; Karazhanov, S.Z.; Hauback, B.C.; Marstein, E.S. On the Crystal Chemistry of Photochromic Yttrium Oxyhydride. *Energies* **2022**, *15*, 1903. https://doi.org/10.3390/en15051903

Academic Editors: Peter Ngene, Adam Revesz and Giovanni Esposito

Received: 11 January 2022
Accepted: 28 February 2022
Published: 5 March 2022

1. Introduction

Photochromic yttrium oxyhydride (YHO) films, first described by Mongstad et al. [1–3], are attractive candidates for many technologically important applications, such as smart windows in buildings and vehicles, and ophthalmology, mainly due to its high transparency in the clear state, its colorfulness and its ability to change color evenly across the visible spectrum. Oxygen plays an important role: it can cause metal-insulator phase transition by transforming the electrically well-conducting oxygen-free yttrium hydride [4,5] to an insulating state [1,2]. It also enables optical band gap engineering [3,6] and an optical phase transition [7,8] by converting the yttrium hydride from opaque into a state of transparency to the visible light [6,7]. Another oxygen-derived phase transition is the conversion of the oxygen-free and optically transparent yttrium hydride [4,5] from a non-photochromic material into a photochromic material [1,2]. Despite the importance of oxygen in the above-mentioned material properties, the atomic structure of the material is still undetermined. More precisely, the site occupied by the oxygen atoms in the crystal structure is unknown.

The chemical formula for oxygen-containing yttrium hydride, Y-H-O is another important issue. Based on first-principles calculations, the chemical formula $YH_{3-2x}O_x$ was proposed [6] and later confirmed experimentally [9]. A phase diagram has been developed for the Y-H-O system, and correlation has been established between the film composition and the photochromic performance of the YHO films [8] that was later confirmed [9] in other oxyhydrides of rare earth metals. The lattices of the Y-H-O system predicted [10] by first-principles calculations are in good agreement with experimental results [8,9]. Although oxyhydride nature has been proposed in Ref. [9], there is no report on diffraction measurements indicating the site preference for the oxide anions. In order to provide insight into the main features of the crystal structure, we performed synchrotron radiation and neutron powder diffraction analysis of the Y-D-O powders that were compared to the results obtained from first-principles calculations [10]. The Y-D-O is an analog of the Y-H-O system in which hydrogen was substituted for deuterium, which is more favorable for neutron diffraction. We report that the oxygen atoms occupy tetrahedral sites in the face-centered cubic (fcc) Y lattice.

2. Materials and Methods

The materials were formed by a two-step fabrication method. In the first step, YD_2 was deposited as a 4 μm thick film on a Cu plate under 1 Pa D_2 (Linde Gas, 99.8% pu-

rity) by reactive magnetron sputtering in a Leybold Optics A550V7 sputter unit operated with a power density of 1:33 Wcm^{-2}. A commercially available Y target of dimensions 125 × 600 × 6 mm^3 with a purity of 99.99% was used. The base pressure in the sputtering chamber prior to film deposition was ~10^{-4} Pa. No O was intentionally introduced into the sputtering chamber. In the second step, the film was oxidized by taking it from the chamber into the air. In this step, oxygen atoms became chemically incorporated into the host metal hydride structure. The thick film delaminated spontaneously during oxidation, forming a coarse powder that was further crushed in a mortar to a fine powder for diffraction measurements.

Synchrotron radiation powder diffraction (SR-PXD) data were collected at the Swiss-Norwegian Beam Lines, BM01, at the ESRF, Grenoble (France). The sample was contained in a 0.5 mm boron glass capillary, which was rotated by 90° during the 30 s exposure to improve powder averaging. The wavelength was λ = 0.7454 Å. The 2D diffraction data were collected on a Pilatus 2M detector and integrated to 1D diffraction patterns with the program BUBBLE [11]. The sample-detector distance was 146 mm.

Powder neutron diffraction (PND) data were collected with the high-resolution diffractometer PUS [12] at the Norwegian Center for Neutron Research (NcNeutron) at IFE, Kjeller (Norway). The sample was contained in a vanadium container with a 6 mm inner diameter. Neutrons with the wavelength λ = 1.554 Å were provided by a vertically focusing a Ge (511) monochromator at a 90° take-off angle. The instrument features two detector banks, each with 7 vertically stacked ^{3}He-filled position-sensitive detector tubes that cover a 20° range in scattering angle. The 2θ range from 10 to 130° was thus covered by moving each detector bank to 3 different positions. Rietveld refinements were performed using Topas Academic version 6 [13]. The Bragg peak shapes were modeled with a Thompson–Cox–Hastings pseudo-Voigt with 2 variables for each dataset. The backgrounds were fitted with a 6-term Chebyshev polynomial. To reduce the number of free parameters, one common displacement factor was used for all anions (O, H and D) in each refinement.

3. Results

The Y-O-D compound crystallizes into a face-centered cubic (fcc) lattice similar to that observed in YH_2, but with an enlarged lattice constant of 5.32 Å, as compared to 5.19 Å for YD_2 [14–16]. The unit cell parameter is in good correspondence with corresponding materials deposited with natural hydrogen [7].

Figure 1a shows the fit for Rietveld refinement with the SR-PXD and an O-free model of expanded YH_2. One can see the mismatch between the relative intensities of the calculated and the observed patterns (weighted R-factor (R_{wp}) = 5.39). In particular, the calculated intensity of the 002 peak is too high compared to the intensities of 111 and 220.

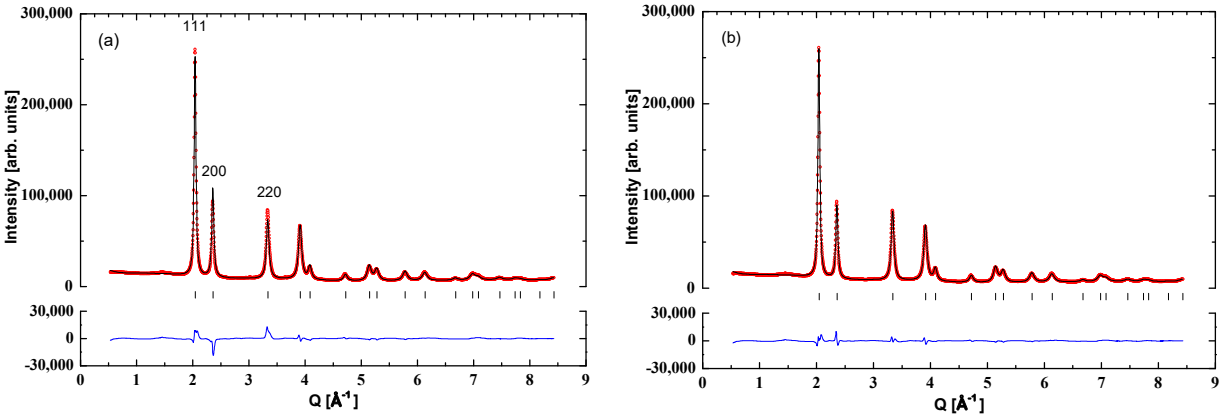

Figure 1. Rietveld refinement with the SR-PXD (λ = 0.7454 Å) for the Y-H-O with O at (**a**) only fcc H atoms (R_{wp} = 5.39) and (**b**) fcc Y with tetrahedral sites partly occupied by O (occ(O) = 0.37, R_{wp} = 3.56).

The inclusion of oxygen has a significant effect on the SR-PXD pattern, despite its weak scattering power compared to the much heavier yttrium. Several models for oxygen inclusion were tested. Oxygen incorporation into the octahedral sites of YD_2 leads to an unphysical negative occupancy factor for oxygen upon refinement, while maintaining significant intensity misfits. A much better fit (R_{wp} = 3.56, Figure 1b) was obtained by allowing O to substitute D on tetrahedral sites i.e., assuming the composition $YD_{2-x}O_x$. The same space group as fcc YH_2 was used, $Fm\bar{3}m$, thus with a disordered distribution of O and D over the tetrahedral sites. The refined composition was $YD_{1.26(2)}O_{0.74(2)}$. No change in R_{wp} occurred when assuming the previously proposed $YD_{3-2x}O_x$ composition (R_{wp} = 3.56). The oxygen content in octahedral and tetrahedral sites were refined independently under the assumption that the tetrahedral sites are fully and disorderly occupied by O and D, while excess D was in octahedral sites. The oxygen occupancy in octahedral sites went to zero during the refinement, while the tetrahedral sites obtained an oxygen occupation very similar to the previous model, thus yielding the composition $YD_{1.48(2)}O_{0.76(2)}$, with about 23% D occupation in octahedral interstices according to the assumed overall composition.

PND data revealed a very high background, thus strongly indicating that the material contains a substantial amount of natural hydrogen (^{1}H) in addition to D, most likely introduced upon reaction with humidity when exposed to air in the second step of the synthesis. Since hydrogen and deuterium have negative and positive coherent neutron scattering lengths, respectively, it is impossible to extract information about the total hydrogen content from the PND data without knowing the H/D ratio in the material. However, it is possible to test the agreement between the PND data and the compositions $Y(H,D)_{2-x}O_x$ and $Y(H,D)_{3-2x}O_x$, where the oxygen occupancy and the H/D ratio are refinable compositional parameter. Rietveld refinements were conducted on the PND and SR-PXD simultaneously, where the weight of the SR-PXD data was reduced by a factor of 0.0001 due to the extreme difference in counting statistics between the two datasets. With this weighting scheme, the two datasets contributed approximately equally to the overall R-factor.

The model with tetrahedral sites fully occupied by anions and empty octahedral sites, $Y(D,H)_{2-x}O_x$, yielded a decent Rietveld fit to the PND pattern with R_{wp} = 2.00 (Figure 2a) and a refined H/D ratio of 1.12(5). The refined composition was $Y(D_{0.502(7)}H_{0.498(7)})_{1.31(1)}O_{0.69(1)}$. The fit to the SR-PXD data was similar to that from the individual refinement (R_{wp} = 3.57). The overall R-factor was 2.34.

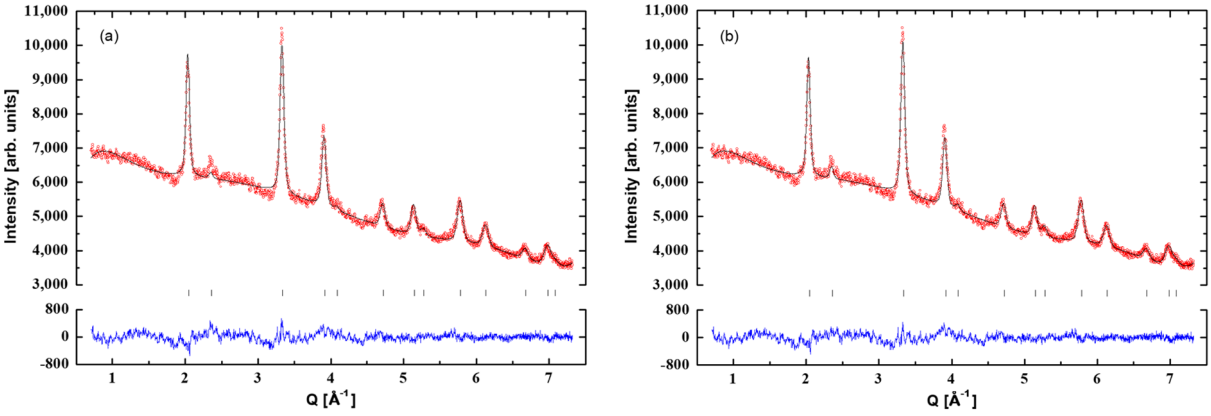

Figure 2. Rietveld fit to PND data (λ = 1.554 Å) from refinement with PND and SR-PXD data for the Y-H-O assuming (**a**) $Y(D,H)_{2-x}O_x$ with anions in tetrahedral sites (R_{wp} = 2.00) and (**b**) $Y(D,H)_{3-2x}O_x$ with additional hydrogen/deuterium in octahedral sites (R_{wp} = 1.95). Note the better fit of the intensity in the second peak (200) with this model.

Determination of the $Y(H,D)_{3-2x}O_x$ composition was attempted next. In a similar manner to the SR-PXD-only refinement, the occupation of oxygen in tetrahedral and octahedral sites was refined independently and the tetrahedral was assumed to be fully occupied by anions. Despite a reasonably small decrease in the R-factor (R_{wp} = 1.93, Figure 2b), the fit to the PND data improved markedly, especially the intensity of the 002, which clearly had too low an intensity with the model with anions only in tetrahedral sites. The refined composition was $Y(H_{0.532(5)}D_{0.468(5)})_{1.66(1)}O_{0.67(1)}$. The R-factor for the SR-PXD fit increased slightly to R_{wp} = 3.59 without any visual deterioration of the fit (Figure S1 in Supplementary Materials). The overall R-factor was R_{wp} = 2.30. The refined parameters for this model are given in Table 1.

Table 1. Refined structure parameters for $Y(H,D)_{3-2x}O_x$ from SR-PXD and PND data. Standard deviations are in parentheses. Isotropic displacement parameters B_{iso}, are constrained to be equal for O, D and H.

Site	Wyckoff Position; Coordinates	Element	Occupation	B_{iso}
Y	4*a*; 0, 0, 0	Y	1	1.27(1)
Tetrahedral site	8*c*; $\frac{1}{4}$, $\frac{1}{4}$, $\frac{1}{4}$	O D H	0.334(7) 0.311(4) 0.354(5)	4.0(1)
Octahedral site	4*b*; $\frac{1}{2}$, $\frac{1}{2}$, $\frac{1}{2}$	D H	0.16(1) 0.18(1)	4.0(1)

Cubic lattice parameter a = 5.3226(3) Å. Space group $Fm\bar{3}m$.

The main driver of charge dynamics in the oxidation process of YH_2 is determined by the yttrium's ability to change the formal ionic charge from 2+ to 3+. It indicates that by creating the only charge transfer channel with yttrium, the incorporated oxygen tends to finalize the yttrium oxidation up to 3+ and thus to provide a firm self-stabilization in the host structure. At the same time, hydrogens are kept in an anionic state free of oxygen impact.

Previous DFT studies have calculated the stability of differently ordered H-O configurations in Y oxyhydrides [10,17]. One of the tested models with lowest energy is *fcc*, and thus it is possible to compare it to the present experimental data. The composition is YOH, and the space group symmetry is $F\bar{4}3m$, with H and O each orderly occupying half of the tetrahedral sites (Figure 3a). Rietveld refinement with this model on our data gives a markedly poorer fit to both the SR-PXD (R_{wp} = 3.73) and PND (R_{wp} = 2.11). The experimental data does therefore not support a long-range ordered distribution of the anions. However, the low energy of the $F\bar{4}3m$ structure may indicate that such H-O configuration shown in Figure 3b may be typical locally in the material due to short-range order.

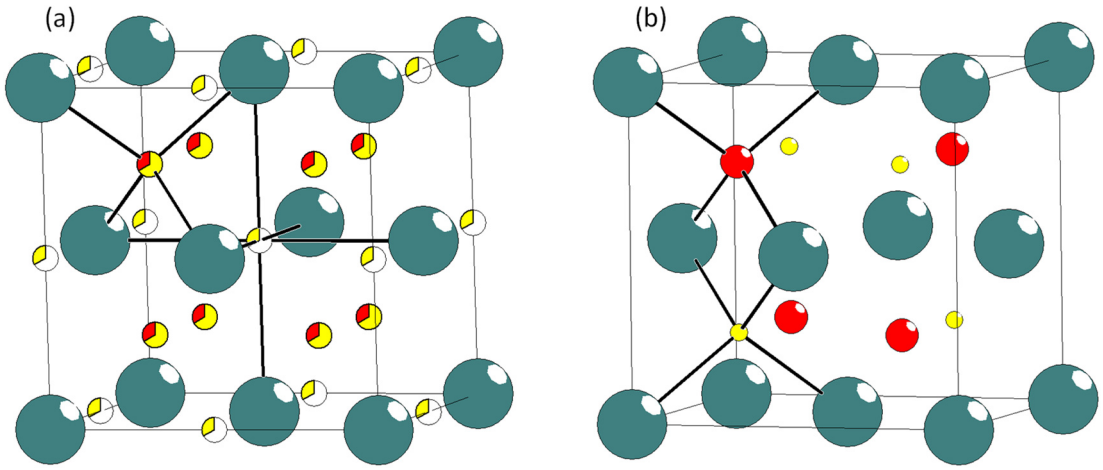

Figure 3. (**a**) Structure model of Y-O-H oxyhydride from combined SR-PXD and PND Rietveld refinement. Size of sectors indicate occupancies in partly or mixed occupied sites. (**b**) Energetically favorable configuration of O and H found in fcc Y-O-H oxyhydride from previous DFT study, which may be prevalent locally in the disordered phase in (**a**). Green: Y; Yellow: H/D; red: O.

4. Conclusions

We investigated the structure of photochromic Y-O-(H,D) oxyhydride with combined Rietveld analysis of SR-PXD and PND data. The Y atoms form an fcc lattice and the oxide anions are located in tetrahedral sites. Due to incorporation of natural hydrogen in the deuterated material, it is difficult to extract certain information about the concentration and location of the hydride anions. However, among the tested models, the composition $Y(H,D)_{3-2x}O_x$ with O and H,D, fully occupying the tetrahedral sites and additional H,D occupying octahedral sites, gives the best fit to the data. The refined composition is $Y(H_{0.532(5)}D_{0.468(5)})_{1.66(1)}O_{0.67(1)}$.

Supplementary Materials: The following supporting information can be downloaded at: https://www.mdpi.com/article/10.3390/en15051903/s1, Figure S1: "Rietveld fit to SR-PXD data from joint refinement with PND data and composition $Y(D,H)_{3-2x}O_x$" CIF for the refined structure model given in Table 1.

Author Contributions: Conceptualization, S.Z.K., B.C.H. and E.S.M.; methodology, F.M. and M.H.S.; formal analysis, M.H.S.; investigation, F.M. and M.H.S.; writing—original draft preparation, S.Z.K. and M.H.S.; writing—review and editing, M.H.S. and S.Z.K.; visualization, M.H.S.; project administration, S.Z.K., B.C.H. and E.S.M.; funding acquisition, E.S.M. and B.C.H. All authors have read and agreed to the published version of the manuscript.

Funding: This research was funded by The Research Council of Norway through IDELAB/NANO2021 (grant 238848) and FRINATEK (grants 287545 and 240477/F20), and through M-ERA.NET (grant 300107).

Institutional Review Board Statement: Not applicable.

Informed Consent Statement: Not applicable.

Acknowledgments: The authors wish to thank the staff at the Swiss–Norwegian beamline (BM01) at the European Synchrotron Radiation Facility (ESRF) in Grenoble, France for skillful assistance during the SR-PXD experiments.

Conflicts of Interest: The authors declare no conflict of interest.

References

1. Mongstad, T.; Platzer-Björkman, C.; Maehlen, J.P.; Mooij, L.P.A.; Pivak, Y.; Dam, B.; Marstein, E.S.; Hauback, B.; Karazhanov, S.Z. A new thin film photochromic material: Oxygen-containing yttrium hydride. *Sol. Energy Mater. Sol. Cells* **2011**, *95*, 3596–3599. [CrossRef]
2. Mongstad, T.T. Thin-Film Metal Hydrides for Solar Energy Applications. Ph.D. Thesis, The University of Oslo, Oslo, Norway, 2012.

3. You, C.C.; Mongstad, T.; Maehlen, J.P.; Karazhanov, S. Engineering of the band gap and optical properties of thin films of yttrium hydride. *Appl. Phys. Lett.* **2014**, *105*, 031910. [CrossRef]
4. Hoekstra, A.F.T.; Roy, A.S.; Rosenbaum, T.F.; Griessen, R.; Wijngaarden, R.J.; Koeman, N.J. Light-Induced Metal-Insulator Transition in a Switchable Mirror. *Phys. Rev. Lett.* **2001**, *86*, 5349–5352. [CrossRef] [PubMed]
5. Hoekstra, A.F.T.; Roy, A.S.; Rosenbaum, T.F. Scaling at the Mott-Hubbard metal-insulator transition in yttrium hydride. *J. Phys.-Condens. Matter* **2003**, *15*, 1405–1413. [CrossRef]
6. Pishtshev, A.; Karazhanov, S.Z. Role of oxygen in materials properties of yttrium trihydride. *Solid State Commun.* **2014**, *194*, 39–42. [CrossRef]
7. Montero, J.; Martinsen, F.A.; Garcia-Tecedor, M.; Karazhanov, S.Z.; Maestre, D.; Hauback, B.; Marstein, E.S. Photochromic mechanism in oxygen-containing yttrium hydride thin films: An optical perspective. *Phys. Rev. B* **2017**, *95*, 201301. [CrossRef]
8. Moldarev, D.; Moro, M.V.; You, C.C.; Baba, E.M.; Karazhanov, S.Z.; Wolff, M.; Primetzhofer, D. Yttrium oxyhydrides for photochromic applications: Correlating composition and optical response. *Phys. Rev. Mater.* **2018**, *2*, 115203. [CrossRef]
9. Cornelius, S.; Colombi, G.; Nafezarefi, F.; Schreuders, H.; Heller, R.; Munnik, F.; Dam, B. Oxyhydride Nature of Rare-Earth-Based Photochromic Thin Films. *J. Phys. Chem. Lett.* **2019**, *10*, 1342–1348. [CrossRef] [PubMed]
10. Pishtshev, A.; Strugovshchikov, E.; Karazhanov, S. Conceptual Design of Yttrium Oxyhydrides: Phase Diagram, Structure, and Properties. *Cryst. Growth Des.* **2019**, *19*, 2574–2582. [CrossRef]
11. Dyadkin, V.; Pattison, P.; Dmitriev, V.; Chernyshov, D. A new multipurpose diffractometer PILATUS@SNBL. *J. Synchrotron Radiat.* **2016**, *23*, 825–829. [CrossRef] [PubMed]
12. Hauback, B.C.; Fjellvåg, H.; Steinsvoll, O.; Johansson, K.; Buset, O.T.; Jørgensen, J. The high resolution Powder Neutron Diffractometer PUS at the JEEP II reactor at Kjeller in Norway. *J. Neutron Res.* **2000**, *8*, 215–232. [CrossRef]
13. Coelho, A.A. TOPAS and TOPAS-Academic: An optimization program integrating computer algebra and crystallographic objects written in C plus. *J. Appl. Cryst.* **2018**, *51*, 210–218. [CrossRef]
14. Vajda, P.; Daou, J.N. Semiconductor-Metal-Semiconductor Transitions in the Superstoichiometric Dihydride Yh2.10. *Phys. Rev. Lett.* **1991**, *66*, 3176–3178. [CrossRef] [PubMed]
15. Uhrich, D.L. Measurement of the Lattice Constant in the Dihydrides of Gadolinium—Yttrium Alloys. *J. Chem. Phys.* **1966**, *44*, 2202–2203. [CrossRef]
16. Khatamian, D.; Kamitakahara, W.A.; Barnes, R.G.; Peterson, D.T. Crystal structure of $YD_{1.96}$ and $YH_{1.98}$ by neutron diffraction. *Phys. Rev. B* **1980**, *21*, 2622–2624. [CrossRef]
17. Baba, E.M.; Montero, J.; Strugovshchikov, E.; Zayim, E.Ö.; Karazhanov, S. Light-induced breathing in photochromic yttrium oxyhydrides. *Phys. Rev. Mater.* **2020**, *4*, 025201. [CrossRef]